$^{45}Sc(d,p)^{46}Sc$ reaction

J. N. Roy,* A. R. Majumder, and H. M. Sen Gupta
Department of Physics, University of Dhaka, Dhaka, Bangladesh
(Received 15 October 1991)

The $^{45}Sc(d,p)$ reaction has been studied at 12 MeV with an overall energy resolution of ~15 keV. The energy levels in ^{46}Sc are obtained up to $E_x \sim 7$ MeV and the angular distributions are measured for most of the levels. The data have been analyzed in terms of the nonlocal finite range distorted-wave Born approximation method and l values and spectroscopic factors are derived.

PACS number(s): 25.55.Hp, 27.40.+z

I. INTRODUCTION

The level structure of the odd-odd nucleus ^{46}Sc has been investigated through various nuclear reactions, namely, $^{43}Ca(\alpha,p\gamma)$, $^{44}Ca(^3He,p)$, $^{45}Sc(n,\gamma)$, $^{45}Sc(d,p)$, $^{45}Sc(t,d)$, $^{46}Ca(^3He,t)$, $^{46}Ti(t,^3He)$, $^{47}Ti(d,^3He)$, and $^{48}Ti(d,\alpha)$ reactions. Information thus obtained is summarized by Alburger [1].

The $^{45}Sc(d,p)^{46}Sc$ reaction was studied by Rapaport *et al.* [2] at 7 MeV and the angular distributions were analyzed for the stripping levels up to $E_x \sim 4$ MeV and only selective levels between $E_x \sim 4$ and 6 MeV. A few levels in ^{46}Sc were observed by Bing *et al.* [3] in the (t,d) reaction in the sub-Coulomb energy ($E_t = 2.2-3.5$ MeV). Although the relative spectroscopic factors in the two reactions are in good agreement between each other, the absolute values are not. Furthermore, several studies have been carried out since the above (d,p) reaction [2] through various reactions leading to a complexity in the level spectrum of ^{46}Sc, as discussed in Sec. IV. The present work on the $^{45}Sc(d,p)^{46}Sc$ reaction was undertaken at a somewhat higher beam energy of 12 MeV so as to reduce any possible compound nuclear effect, since the Q value of the (d,p) reaction on ^{45}Sc is only about 1.6 MeV lower than that of the (d,n) reaction.

Angular distributions are measured for most of the levels up to $E_x \sim 7$ MeV. Detailed distorted-wave Born approximation (DWBA) analyses were carried out, which included a spin-orbit term in the bound state potential; the importance of such a term has been emphasized in the literature (Ref. [3], for example). An unambiguous assignment of l transfer was made to most of the stripping angular distributions and the spectroscopic factors are extracted.

II. EXPERIMENTAL PROCEDURE

The experiment was carried out with a beam of 12 MeV deuterons obtained from the Tandem Van de Graaff accelerator of the Nuclear Physics Laboratory, University of Oxford, Oxford. The target was prepared by the vacuum deposition of natural scandium onto thin carbon backing. The target was placed at the center of a multigap magnetic spectrograph and was continuously monitored during the experiment against any deterioration. The target was slightly displaced both horizontally and vertically from time to time so as to expose a small region of it about its center. The monitor showed a variation no more than 5%, thus showing the uniformity in the thickness. The reaction products were momentum analyzed in a magnetic field of strength 9.06 kG and only protons were recorded in Ilford L4 emulsion 25 μm thick placed at the focal plane of the spectrograph simultaneously over the angles 11.25°–116.25° (laboratory) in steps of 7.5°. Particles other than protons were stopped in polythene foils placed on top of the plates. The total beam charge was 3500 μC.

The plates were scanned at Dhaka and the energy spectrum was obtained at each angle. A typical spectrum is shown in Fig. 1. The energy resolution (FWHM) was ~15 keV. A total of 201 levels were obtained, including a few unresolved ones, up to $E_x \sim 7$ MeV. The criteria used for the identification of levels were that the excitation energies of a level at different angles agreed to within about 10 keV and that a level had similar widths at different angles. The excitation energies were obtained from an internal calibration of the spectrograph by a least-squares parabolic fit to several well known levels in ^{46}Sc, shown underlined in Table I, as well as to a few contaminant lines. The latter served as useful reference lines at excitation energies where the level density is extremely high. Also included in the table are the energy levels given in the previous (d,p) work [2] and those summarized in the data sheets [1]. Repeated scanning of the plates were done for the following: (a) Levels for which the l_n assignments in the present work disagreed with those of Rapaport *et al.* [2] as well as with the adopted J^π values, (b) levels having contradictory J^π values or limits from various reactions, and (c) levels sitting on a rather large background ($E_x > 4.5$ MeV).

Special care was taken for groups standing on a rather large background and weak groups appearing on the shoulder of a strong group, as well as groups appearing as

*Present address: The Medical Center, University of California, San Francisco, CA 94143.

TABLE I. Summary of the $^{45}Sc(d,p)^{46}Sc$ reaction. NA, data not analyzed; see text. NS, nonsingle step process. Peak cross section where not shown is less than 10 μb/sr, if not under contaminant.

Group	E_x (MeV)			$\sigma_{max}(\theta)$	l transfer		$(2J_f+1)C^2S$		J^π
	a	b	c	(mb/sr)	a	b	a	b	c
0	0.0	0.0	0.0	0.32	3	3	2.82	4.64	4^+
1	0.046	0.051	0.052	0.80	3	3	6.90	10.64	6^+
2	0.145	0.140	0.143	~0.005	NA				1^-
3	0.226	0.227	0.228	0.30	3	3	2.86	4.96	3^+
4	0.280	0.279	0.281	0.71	1+3	1[d]	0.44+4.29	0.80[d]	5^+
			0.290						2^-
5	0.447	0.444	0.444	0.15	3	3	1.60	2.48	2^+
6	0.588	0.577	0.585	~0.002	NA				3^-
7	0.634	0.623	0.627	~0.002	NA				4^-
8	0.773	0.772	0.774	0.36	3	3	2.78	4.88	5^+
9	0.837	0.833	0.835	0.20	3	3	1.68	2.56	4^+
10	0.980	0.975	0.977	0.48	3	3	3.39	4.00	7^+
11	1.006		0.991	0.17	3		1.07		1^+
12	1.093	1.090	1.089	0.24	1	1	0.13	0.24	4^+
13	1.131	1.131	1.124	0.055	0	(0)	0.027	0.008	4^-
14	1.143	1.141	1.141	0.028	0	(3)	0.036	0.24	
15	1.275	1.271	1.270	~0.002	NA				4^-
			1.298						
16	1.326	1.323	1.321	0.045	3	(1)	0.39	0.32	$3^+,(4^+)$
17	1.399	1.394	1.394	0.045	1	1	0.045	0.48	2^+
18	1.441	1.435	1.428	0.010	0	(1)	0.071	0.008	(2^+)
19	1.528	1.526	1.527	0.008	NA				$(2^-,3,4^+)$
20	1.648	1.648	1.643	0.033	0	0	0.017	0.040	4^-
21	1.675	1.677	1.677	0.39	1	1	0.16	0.24	
		1.692	1.692			0			3^-
22	1.716	1.708	1.708	~0.005	NA				$3^-,2^-$
23	1.753	1.753	1.753	0.008	(3)	(3)	0.59	0.24	
24	1.774	1.765	1.763	0.12	1	(1)	0.051	0.04	$2^+,3^+,4^+$
25	1.805	1.803	1.779	0.67	1	1	0.32	0.40	2,3
26	1.826	1.824	1.824						
27	1.852	1.851	1.852	0.037	1	NS	0.016		1^+
28	1.879	1.890	1.886	0.19	3	1	1.17	0.11	$3^+,(2^+)$
			1.920						2^+
29	1.920	1.925		0.090	NS	1		0.14	
			1.921						
			2.043						$3^-,(2^-)$
30	2.059	2.059	2.062	0.031	NA	(0)		0.13	$(4)^-$
31	2.074	2.071	2.070	1.71	1	1	0.84	0.80	(3^+)
			2.084						
			2.114						3,4(2)
32	2.116	2.118		2.40	1	1	1.10	0.14	
			2.119						$3^+,(4^+)$
33	2.177	2.174	2.185			NA			
34	2.211	2.208	2.203	0.022	3		0.15		3^-
35	2.224	2.225	2.222	0.70	1	1	0.23	0.40	2^+
			2.253						
36	2.295	2.296	2.292	NA					
37	2.306	2.307	2.303	0.43	1	1	0.23	0.48	$2^+,3^+,(4^+)$
38	2.329	2.334	2.330	9.88	1	1	4.94	6.40	
			2.367						
39	2.375	2.366		0.12	(1)	1	0.086	0.056	
			2.375						
			2.396						
40	2.415	2.410	2.410	0.96	1	1	0.40	0.48	3^+
			2.431						$(4^+,5^+)$
			2.442						3^+
			2.451						
41	2.455	2.455	2.460	2.30	1	1	1.00	1.44	3^+

TABLE I. (*Continued*).

Group	E_x (MeV)			$\sigma_{max}(\theta)$	l transfer		$(2J_f+1)C^2S$		J^π
	a	b	c	(mb/sr)	a	b	a	b	c
			2.486						
			2.494						
42	2.535	2.533	2.522	1.50	1	1	0.65	0.88	
			2.559						4^+
43	2.564	2.566	2.568	2.35	1	1	1.00	1.28	$3^+,4^+$
44	2.594	2.590	2.590	0.055	2	(0)	0.13	0.008	$3^-,4^-$
45	2.651	2.648	2.643	0.027	(2)	(0)	0.067	0.008	$3^-,4^-(2^-)$
46	2.673	2.670	2.663	0.048	1		0.025		
			2.695						3
			2.705						3^+
47	2.712	2.716	2.714	4.12	1	1	1.67	1.92	
		2.733	2.733						2^+
48	2.760			0.055	1		0.032		
49	2.790	2.780	2.783	0.43	0	0	0.12	0.11	$3^-,4^-$
50	2.817	2.813	2.813	0.46	1	1	0.22	0.28	1^+
51	2.844	2.837	2.834	0.059	(1)	0	0.029	0.032	
			2.856						2,3,4
52	2.863	2.862	2.863	5.09	1	1	2.17	2.48	$2^+,(3^+)$
53	2.898	2.897	2.891	0.46	1	1	0.22	0.32	
54	2.945	2.939	2.940	0.093	0	(0)	0.031	0.008	
			2.957						
55	2.978	2.982	2.980	2.38	1	1	1.05	1.40	$3^+,4^+$
		3.005	3.002						
		3.021	3.017						$4(3^+,4^+)$
56	3.034	3.032	3.032	1.21	1		0.43		
57	3.064	3.061	3.057	1.78	1		0.63		
			3.082						
58	3.093	3.087	3.095	1.01	1	1	0.45	0.10	$3^+,4^+,(2^+)$
			3.116						1^+
59	3.144	3.142	3.136	0.24	(0)	0	0.039	0.04	$3^-,4^-$
60	3.184	3.183	3.177	1.55	1	1	0.41	0.64	4^+
			3.192						$(2^+,3^+)$
			3.205						
			3.230						$2^+,3^+,4^+$
61	3.244	3.241	3.240	1.30	1	1	0.60	0.88	$0^+,1^+$
			3.260						
62	3.282	3.287	3.279	0.022	NS	1		0.064	$2^+,3^+$
			3.314						4^+
63	3.325	3.321	3.338	0.67	1	1	0.32	0.37	
			3.381						
64	3.397	3.391	3.397	1.14	1	1	0.52	0.80	$2^+,3^+,(4^+)$
			3.414						$2^+,3^+,4^+$
65	3.424	3.420	3.425	0.94	1	1	0.52	0.60	$3^+,(4^+)$
66	3.450	3.449	3.443	1.20	1	1	0.55	0.66	$2^+,3^+,4^+$
67	3.482	3.480	3.474	0.59	1	1	0.24	0.35	$3^+,4^+(2^+)$
			3.493						2^+
68	3.514	3.509	3.509	0.55	1	1	0.25	0.34	
69	3.537	3.539	3.550	1.57	1	1	0.65	0.80	$2^+,3^+,4^+$
70	3.589	3.586	3.597	0.03	NS	1		0.064	$2^+,3^+,4^+$
71	3.612	3.618	3.605	1.77	1	1	0.72	0.92	
			3.620						
			3.631						$3^+,4^+,5^+$
72	3.660	3.661	3.655	0.31	1	1	0.14	0.22	
			3.675						4
73	3.696	3.695	3.707	0.43	1	(1)	0.21	0.16	$3^+,4^+,(2^+)$
74	3.729	3.715	3.721	0.079	(1)	(1)	0.038	0.12	
75	3.768	3.771	3.767	1.79	1	1	0.82	0.77	3^+
76	3.787	3.792	3.785	0.44	1	1	0.20	0.29	4^+

TABLE I. (*Continued*).

Group	E_x (MeV)			$\sigma_{max}(\theta)$	l transfer		$(2J_f+1)C^2S$		J^π
	a	b	c	(mb/sr)	a	b	a	b	c
77	3.813	3.822	3.814	0.50	1	1	0.22	0.25	
78	3.835	3.839	3.841	0.10	1	(1)	0.042	0.12	$3^+,4^+$
			3.869						
79	3.876	3.878	3.877	0.64	1	(1)	0.29	0.46	$3^+,4^+$
80	3.931	3.941	3.937	0.31	1	1	0.14	0.30	
			3.945						
81	3.961	3.960	3.960	0.078	1	(1)	0.074	0.11	
82	3.986	3.980	3.980	0.010	1	(1)	0.10	0.22	
83	4.005	4.010	4.010	0.40	1		0.16		
84	4.028	4.030	4.040	0.15	1		0.035		
85	4.066	4.070	4.075	0.11	(1)		0.035		
86	4.083	4.082	4.081	1.41	(1)		0.31		
87	4.120	4.120	4.104	0.53	NA				
		4.136	4.132						
88	4.153		4.143	0.29	2		0.52		
		4.185	4.185						$0^+,1^+$
89	4.186			0.40	NS				
90	4.198								
		4.201	4.201						
91	4.224	4.233	4.233	0.21	3		1.55		
92	4.248	4.250	4.250		NA				
		4.270	4.261						
						(1)		0.53	
93	4.284	4.292	4.295	0.28	1		0.15		
94	4.304	4.318	4.319	0.25	1		0.17		
95	4.332	4.327	4.327	0.49	NS				
96	4.353	4.347	4.362	0.21	3		0.13		
97	4.385	4.376	4.383	1.84	1	(1)	0.81	0.92	
98	4.403	4.395	4.395		NS	NS			
			4.414						
99	4.434	4.436	4.433		NS				
100	4.448	4.452	4.448		NS				
101	4.464	4.476	4.467	1.06	1	1	0.43	0.74	
102	4.490	4.505	4.505	0.96	1	1	0.37	0.65	
103	4.518		4.523	0.81	1	1	0.27		
104	4.540	4.537	4.529		NA				
105	4.560		4.559		NA				
106	4.570	4.579	4.579	0.64	1		0.21		
107	4.590	4.594	4.587	1.10	NS				
108	4.619	4.612	4.606	0.82	1		0.30		
109	4.651	4.646	4.646	0.18	1		0.24		
110	4.669	4.662	4.662	0.52	1		0.26		
111	4.690	4.688	4.695	1.02	1		0.52		
			4.701						
112	4.716	4.710	4.720		NA				
113	4.734	4.730			NA				
114	4.756	4.754	4.754	1.19	1	(1)	0.35	0.80	
115	4.770		4.761		1		0.064		
		4.780	4.787						$0^+,1^+$
116	4.793	4.795	4.795	0.58	0		0.15		
117	4.816	4.819	4.819	0.38	NA				
118	4.848	4.844	4.844	2.02	1		0.77		
119	4.869	4.872	4.873		NA				
120	4.881		4.883		NA				
121	4.898	4.894		1.171	1		0.65		
122	4.928	4.925	4.925	0.50	2		0.84		
123	4.957	4.954	4.961						

TABLE I. (*Continued*).

Group	E_x (MeV)			$\sigma_{max}(\theta)$	l transfer		$(2J_f+1)C^2S$		J^π
	a	b	c	(mb/sr)	a	b	a	b	c
				0.70	1		0.25		
124	4.973	4.970	4.970						
125	5.011	5.008	5.008	0.81	1	(1)	0.28	0.50	
126	5.026	5.022	5.021						0^+
127	5.046	5.043	5.049	0.36	1		0.11		
128	5.059	5.062	5.062		NS	NS			
129	5.075	5.082	5.093	1.01	1+3		0.36+6.62		
130	5.110	5.115	5.115	0.89	1		0.32		
131	5.131	5.139	5.139		NA				
132	5.146	5.152	5.152	0.97	0		0.18		
133	5.162	5.167	5.164	1.02	1		0.37		
134	5.190	5.194	5.197						
				2.48	1		0.73		
135	5.205	5.208	5.208						
136	5.232	5.237	5.237		NA	1		0.51	
137	5.250	5.250	5.250	0.22	3		0.60		
138	5.272	5.272	5.272		NA				
139	5.298	5.301	5.302	0.94	NS				
140	5.326	5.327	5.327		NA				
141	5.343	5.345	5.346	0.67	0		0.13		
142	5.363	5.365	5.365	0.33	NS				
143	5.376	5.376	5.376		NA				
144	5.389	5.387	5.387		NA				
145	5.402	5.405	5.405	1.45	1		0.69		
146	5.427			1.00	1		0.30		
147	5.448	5.441	5.441	0.24	1		0.11		
148	5.465	5.465	5.465	0.40	NS				
149	5.491			0.12	(3)		0.52		
150	5.510	5.517	5.517	0.62	1		0.30		
151	5.527	5.529	5.541						
152	5.561	5.565	5.565	0.67	0		0.12		
153	5.597	5.596	5.593	0.62	1		0.22		
154	5.620	5.619	5.619	0.71	1		0.31		
		5.644	5.644						
155	5.656	5.662	5.662	0.99	1	1	0.36	0.37	
156	5.691	5.696	5.696	1.70	NA				
						1		0.38	
157	5.725	5.729	5.729	0.94	NS				
158	5.753	5.753	5.753	0.49	3		0.98		
159	5.773	5.771	5.771	0.46	1		0.13		
160	5.796	5.796	5.796		NA				
161	5.814	5.813	5.813	0.88	1		0.25		
162	5.839	5.835	5.835	0.98	1		0.26		
163	5.877	5.878	5.878	0.57	1		0.18		
164	5.907	5.908	5.908	0.18	NS				
165	5.925	5.930	5.930	0.63	1		0.16		
166	5.958	5.951	5.951	0.23	NS				
167	5.982	5.976	5.978	0.34	(1)		0.10		
168	6.004			0.88	1		0.26		
169	6.037			0.36	1+3		0.13+1.74		
170	6.061			0.52	1		0.17		
171	6.083			0.51	1		0.13		
172	6.110			0.39	1		0.11		
173	6.134								
174	6.145			0.50	1		0.20		
175	6.159			0.90	1		0.21		
176	6.191			0.76	3		2.58		
177	6.253			0.12	NS				

TABLE I. (*Continued*).

Group	E_x (MeV)			$\sigma_{max}(\theta)$	l transfer		$(2J_f+1)C^2S$		J^π
	a	b	c	(mb/sr)	a	b	a	b	c
178	6.276			0.68	1		0.20		
179	6.295			0.35	3		1.19		
180	6.327			0.35	NS				
181	6.362			0.29	1		0.11		
182	6.380			0.17	1		0.063		
183	6.405			0.36	3		1.44		
184	6.429			0.21	1		0.12		
185	6.454			0.22	1		0.073		
186	6.469			0.44	1		0.14		
187	6.482			0.21	NS				
188	6.497			0.14	1		0.064		
189	6.525			0.22	1		0.085		
190	6.549			0.42	1		0.089		
191	6.568			0.12	NS				
192	6.593			0.15	NS				
193	6.612			0.54	1		0.14		
194	6.650			0.49	1		0.14		
195	6.682				NA				
196	6.698				NS				
197	6.728			0.36	NS				
198	6.762			0.25	NS				
199	6.810				NA				
200	6.853				NA				
201	6.874				NA				

[a]Present work.
[b] Rapaport *et al.* [2].
[c]Summary by Alburger [1].
[d]A reanalysis of the angular distribution by Bing *et al.* [3] required $l=1+3$ with the respective strengths of 0.32 and 3.2.

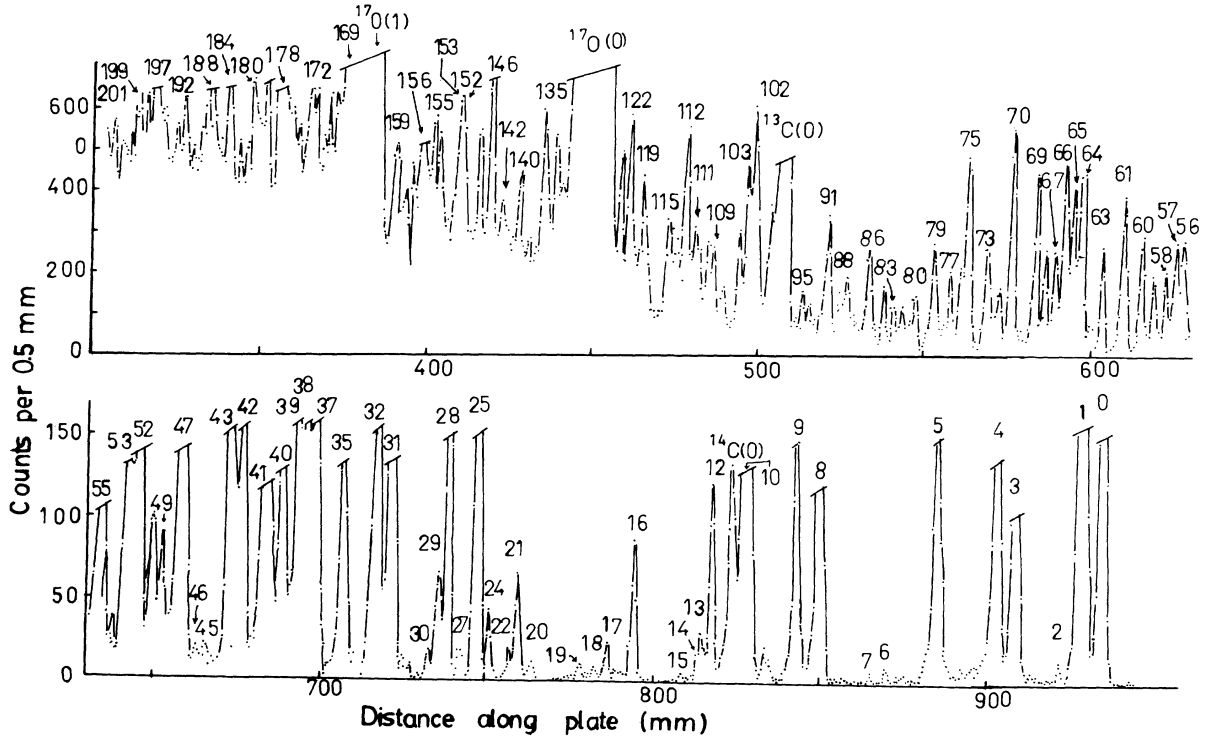

FIG. 1. Energy spectrum of protons at a laboratory angle of 41.25°.

close doublets. In the latter two cases, the area under a peak was determined by using a data extraction routine based on two Gaussian fits to the spectrum including background substraction [4]. In determining the area in all the cases the background was assumed to be either linear or parabolic; the difference, however, turned out to be insignificant. Levels for which repeated extraction gave yield not agreeing to one another within statistics were excluded from data analysis.

To measure the target thickness, a subsidiary short exposure of 0.92 μC was taken on the elastic scattering of 3 MeV deuterons from the same target as used in the main experiment under a magnetic field of strength $\sim$5.48 kG. The target was again displaced only slightly horizontally and vertically as in the main experiment. The yield of the elastic group at 26.25° was normalized to the Rutherford cross section and the target thickness was found to be 53 ± 3 μg cm^{-2}. Error in the absolute cross section of the (d,p) reaction, arising mostly from the uncertainties in the target thickness and background subtraction, was estimated to be less than 15%.

III. DWBA ANALYSIS

The DWBA calculations were carried out using the code DWUCK4 due to Kunz. The optical model potential was of the form

$$V(r)=V_0 f(r,r_0,a)+i4W_D a_I(d/dr)f(r,r_I,a_I)+2\left[\frac{\hbar}{m_\eta c}\right]^2 V_{\text{s.o.}}\, r^{-1}(d/dr)\times f(r,r_{\text{s.o.}},a_{\text{s.o.}})\mathbf{l}\cdot\mathbf{s}+V_C(r)\ ,$$

where

$$f(r,r_0,a)=[1+\exp(r-r_0A^{1/3})/a]^{-1}\ ,$$

and $V_C(r)$ is the Coulomb potential due to a uniformly charged spherical nucleus of radius $R_c=r_cA^{1/3}$. The remaining symbols carry their usual meaning. The bound state wave function was generated by using the real Woods-Saxon potential including a Thomas-Fermi spin-orbit potential, with geometrical parameters shown in Table II. The strength of the potential was adjusted so as to reproduce the appropriate binding energy. Effects of the finite range of the n-p interaction and the nonlocality of the optical model potentials were included in the local energy approximation with the range parameter of 0.621 fm and the range of nonlocality $\beta_d=0.54$ fm and $\beta_n=\beta_p=0.85$ fm (Seth *et al.* [5]).

The spectroscopic factors were extracted using the relation

$$\sigma_{\text{exp}}(\theta)=1.55\left[\frac{2J_f+1}{2J_i+1}\right]\left[\frac{\sigma_{\text{DW}}(\theta)}{2j+1}\right]C^2S\ ,$$

where J_i and J_f are, respectively, the angular momentum in the initial and final levels and j is the angular momentum of the transferred neutron. The optical model parameters [6–10] are listed in Table II.

To begin with, detailed DWBA analyses were carried out for transitions to the following strongly excited levels in ^{46}Sc using various sets of potential parameters in both the entrance and exit channels

$l=3$: 0.0, 0.046, and 0.773 MeV ,

$l=1$: 2.116, 2.329, 2.455, 2.712 ,

and 2.863 MeV .

Some of the DWBA fits are shown in Fig. 2. An overall good description of the angular distributions of the levels under study (three $l=3$ and five $l=1$ transitions, as above) is given by the combinations $D2$-$P2$ and $D3$-$P3$, the former being somewhat better than the latter. An unambiguous assignment of l values is thus possible (Fig. 2). All subsequent DWBA analyses were carried out using the combination $D2$-$P2$ with the expectation that this combination will also lead to an unambiguous l assignment to the levels at higher excitation. This expectation is indeed borne out for most cases (Sec. IV).

The spectroscopic factors are known to depend on the parameters of the optical model used in the DWBA analyses. The use of different combinations of parameter sets giving "acceptable" fits to the angular distributions of the levels mentioned above in our work led to a variation of about 20% in the C^2S values for $l=3$ transfers and about 12% for $l=1$ transfers. The variation increases if we include the combinations fitting only the main stripping peak; the fit becomes unsatisfactory at larger angles. This

TABLE II. Optical model parameters.

Particle notation	V_0 (MeV)	r_0 (fm)	a (fm)	$4W_D$ (MeV)	r_I (fm)	a_I (fm)	$V_{\text{s.o.}}$ (MeV)	$r_{\text{s.o.}}$ (fm)	$a_{\text{s.o.}}$ (fm)	r_c (fm)	Ref.
Deuteron											
$D1$	106.0	1.05	0.85	44.0	1.59	0.40	7.0	0.90	0.60	1.30	[6]
$D2$	89.34	1.175	0.752	68.24	1.351	0.627				1.30	[7]
$D3$	99.4	1.07	0.832	45.20	1.41	0.73	12.0	1.07	0.832	1.30	[8]
Proton											
$P1$	53.2	1.18	0.60	25.2	1.24	0.70	6.4	0.85	0.47	1.29	[9]
$P2$	50.2	1.24	0.59	31.2	1.20	0.59	6.5	0.94	0.54	1.29	[9]
$P3$	53.12	1.17	0.75	38.4	1.32	0.56	6.2	1.01	0.75	1.17	[10]
Neutron	a	1.25	0.65				$\lambda=25$	1.01	0.75		

[a]The depth is adjusted to give a binding energy equal to the separation energy.

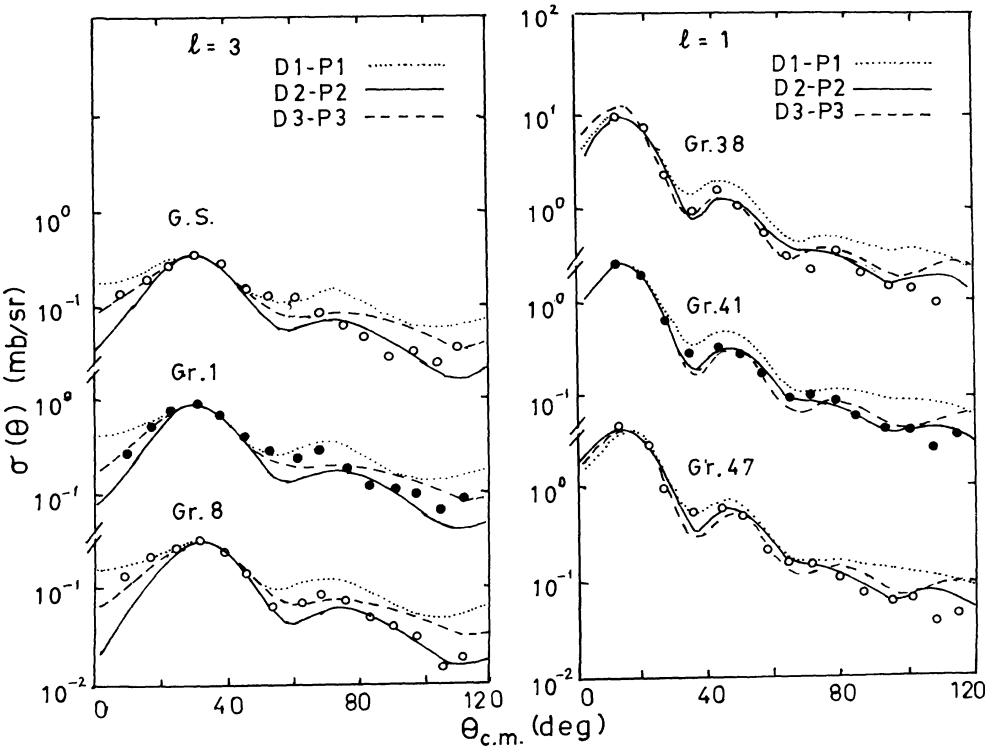

FIG. 2. DWBA fits to some of the angular distributions using different combination of potential parameters of Table II.

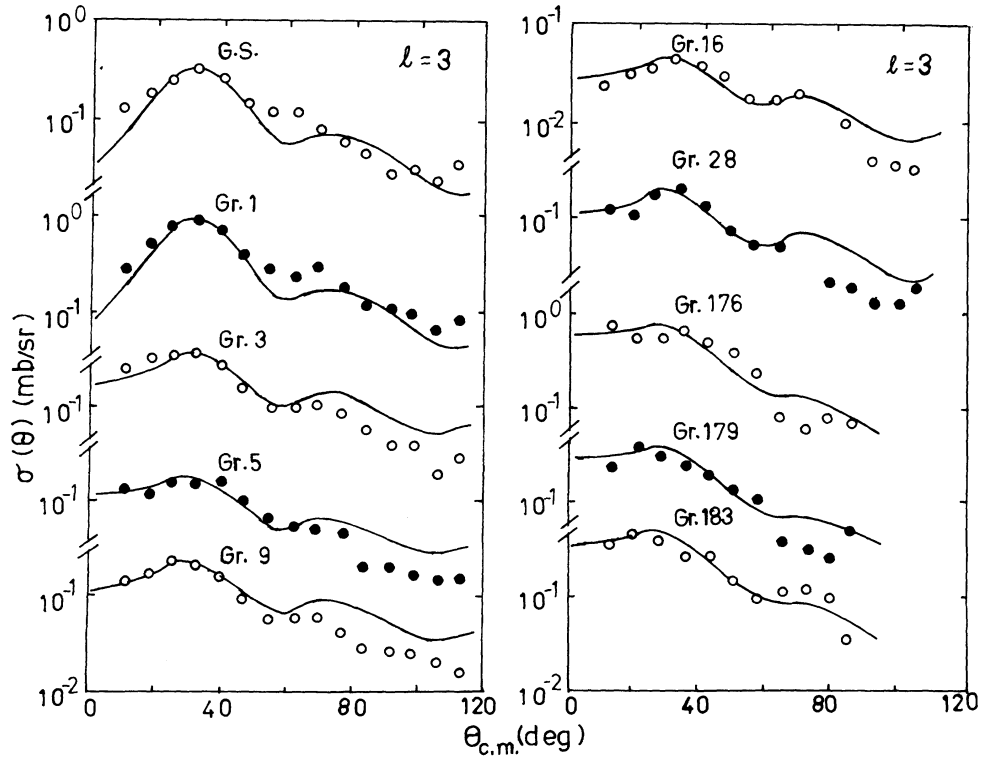

FIG. 3. Measured angular distributions fitted with $l=3$ DWBA curves.

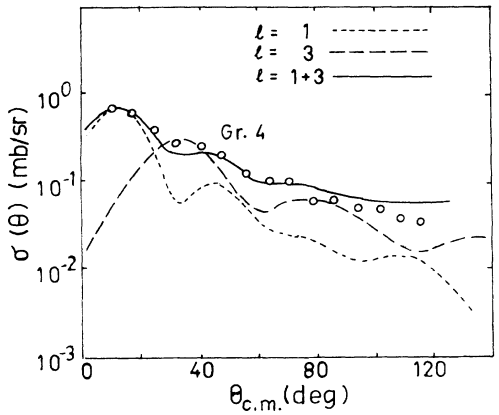

FIG. 4. Measured angular distributions fitted with $l=1+3$ DWBA curves.

is of course usual of all DWBA calculations. The total uncertainty in the transition strength (from both absolute values of measured cross sections and the inherent uncertainty in the DWBA values) is about 30%.

The importance of the spin-orbit term in the bound state potential is again noted, as in Refs. [3] and [11], while the spin-orbit term in the deuteron potential was again found to have very little effect on the DWBA cross sections.

IV. RESULTS AND DISCUSSION

The angular distributions showing predominantly a stripping character are compared with the DWBA calculations. Results are summarized in Table I. Also included in the table are the results from the previous $^{45}Sc(d,p)^{46}Sc$ reaction studied by Rapaport *et al.* [2] and the summary on the level spectroscopy of ^{46}Sc from various reactions (Alburger [1]).

Typical examples of the DWBA fits to the measured angular distributions are shown in Figs. 3–7. A few angular distributions could not be fitted by a single l transfer. A mixture of two l values was considered only when a definite improvement in the quality of fit was thereby attained and the higher l component had an appreciable contribution to the cross section. The proportion of each component was determined from a least-squares fit to the measured angular distribution. A typical distribution ($l=1+3$) is shown in Fig. 4.

Levels for which the cross section data are missing at the extreme two forward angles, due either to the presence of a contaminant or to an emulsion disturbance, are excluded from the DWBA analysis. Such levels are marked NA in Table I. Also excluded from the analysis are the levels for which the cross section data from repeated extraction did not agree within statistics. These levels are usually weak and/or standing on a rather large background. There are also marked NA in the table.

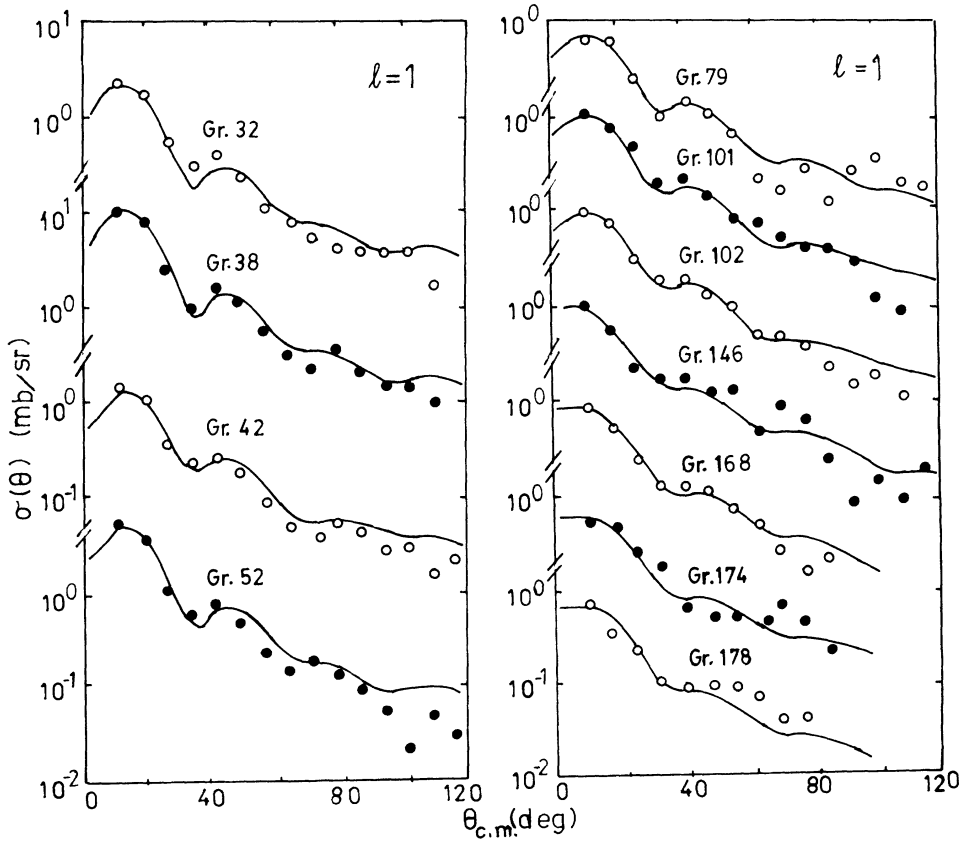

FIG. 5. Measured angular distributions fitted with $l=1$ DWBA curves. Error bars in this and the following figures are statistical.

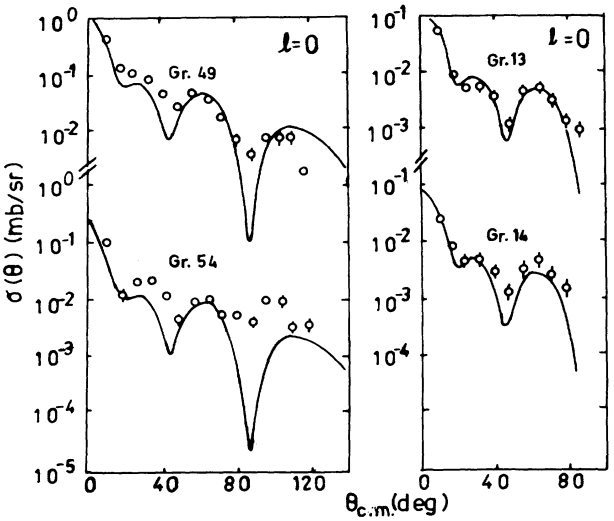

FIG. 6. Measured angular distributions fitted with $l=0$ DWBA curves.

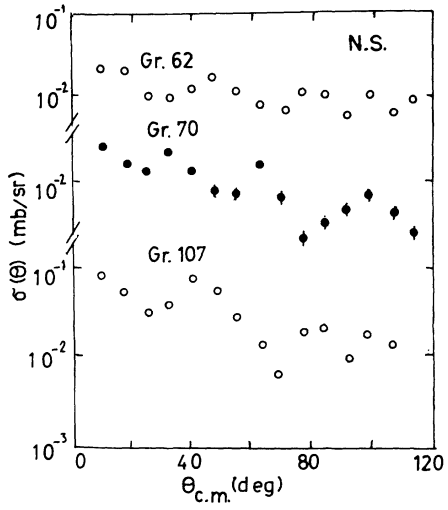

FIG. 8. Angular distributions of the levels designated NS in Table I.

Angular distributions to some of the levels are found to have very little or even no falloff in cross section with increasing angle. The levels are usually weak and the distributions could not be fitted with a single l or a mixture of two l transfers. It thus seems possible that these are populated through a multistep (NS) process. We tentatively assign NS to these levels (Table I). Typical examples are shown in Fig. 8.

The single particle strengths are heavily fragmented over a number of levels as shown in Fig. 9. Results of the sum rule analyses are summarized in Table III. Results from the earlier (d,p) reaction on ^{45}Sc (Rapaport *et al.* [2]), as well as on the isotonic nuclei ^{44}Ca and ^{46}Ti (Refs. [12–14], are also shown.

The spectroscopic factors obtained in the present work, level by level, are usually smaller than those given in the previous (d,p) reaction [2], but agree reasonably well with those given for some selected transitions studied in the (t,d) reaction [3]. The summed strengths in our work are, however, larger than those in Ref. [2], because many more transitions are seen in the present experiment than by Rapaport *et al.* [2].

Discussions on the different l transitions are made below.

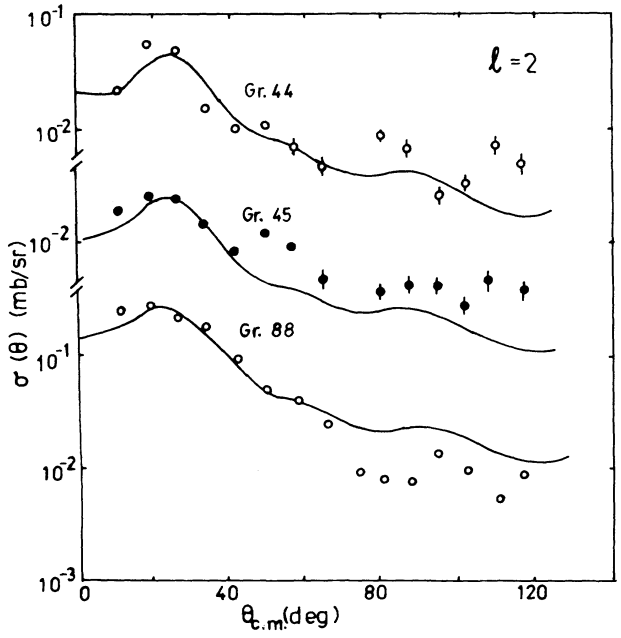

FIG. 7. Measured angular distributions fitted with $l=2$ DWBA curves.

A. The $l=3$ transitions

The $l=3$ transitions are characterized by two regions of excitation (Fig. 9) clearly separated from each other, one with $E_x \lesssim 2$ MeV and the other with $E_x > 4$ MeV, and it is reasonable to assume that these correspond to the $1f_{7/2}$ and $1f_{5/2}$ shells. The corresponding summed spectroscopic strengths, $\sum(2J_f+1)C^2S/(2J_i+1)$, are found to be respectively ~ 3.7 and ~ 2.2 (Table III). The former value within error is consistent with the shell model limit of 4, while the latter is less than 40% of the expected $1f_{5/2}$ strength. The major part of the $1f_{5/2}$ shell model strength thus lies at $E_x > 4$ MeV. The centers of gravity of the $f_{7/2}$ and $f_{5/2}$ shells are, respectively, at 0.50 and > 5.5 MeV.

In contrast to the heavy fragmentation of the $l=3$ transition strength in the ^{45}Sc(d,p)^{46}Sc reaction (because of the residual n-p interaction) the entire $1f_{7/2}$ strength in the ^{44}Ca(d,p)^{45}Ca reaction is carried by the g.s. transition without fragmentation and only two $1f_{5/2}$ levels are found below $E_x \sim 6$ MeV carrying only about 20% of the shell model strength [12]. In the (d,p) reaction on another isotonic nucleus, namely ^{46}Ti, the $1f_{7/2}$ shell model strength is shared among five or six levels with a good

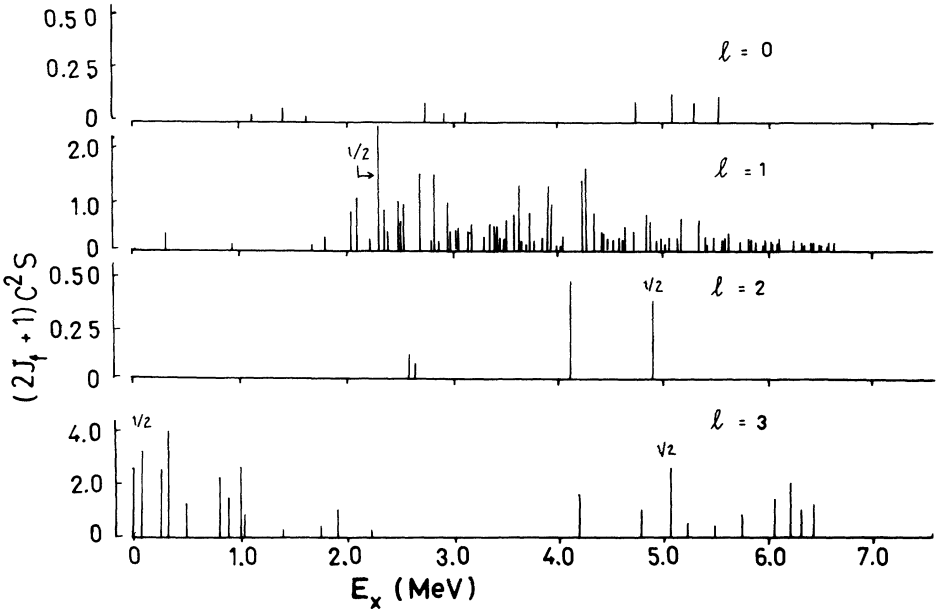

FIG. 9. Distribution of the single particle strengths among the components of a shell model state.

amount (about 50%) concentrated on the first excited level and the $1f_{5/2}$ strength is far from exhausted up to $E_x \sim 7.2$ MeV [13,14].

Several new $l=3$ transitions are identified in the present work, namely $E_x = 1.006$, 2.211, 4.224, 4.353, 5.250, 5.491, 5.753, 6.037, 6.191, 6.295, and 6.405 MeV, the angular distributions of which were either not measured or not analyzed or in some cases, the levels were not observed by Rapaport *et al.* [2]. Some of the angular distributions together with the DWBA fits are shown in Fig. 3.

The $l=3$ assignments to some of the level in the present work are in disagreement with the assignments by Rapaport *et al.* [2]. The levels at $E_x = 1.326$ and 1.879 MeV according to these authors are characterized by the $l=1$ transfer (the former tentatively); the distributions in our work are reasonably well given by $l=3$ (Fig. 3). The most noticeable discrepancy is for the transition to the 0.280 MeV level. The present assignment, in agreement with the (t,d) reaction [3], is $l=1+3$ (the DWBA fit is shown in Fig. 4), which is in disagreement with the $l=1$ of Rapaport *et al.* [2]. A reanalysis of their (d,p) angular distribution by Bing *et al.* [3] indeed gives a better fit to the data with $l=1+3$ than with the original $l=1$ alone. As discussed below, this is identified as the missing 5^+ member of the multiplet having the shell model configuration $[\pi(f_{7/2})\nu(f_{7/2})]$.

Extensive shell model calculations have been carried out by McCullen *et al.* [15] (also termed as the MBZ model) for nuclei in this region of the periodic table. The model is based on an inert ^{40}Ca core with the extra-core nucleons restricted only to the $1f_{7/2}$ shell. A multiplet of

TABLE III. Sum rule analysis of the (d,p) transition strength $(2J_f+1)C^2S/(2J_i+1)$.

Single particle state	^{45}Sc a	^{45}Sc b	^{44}Ca c	^{46}Ti d	^{46}Ti e	f
$2s_{1/2}$	0.043[g]	0.024	0.11	0.15	0.13	0
$1d_{3/2}$	0.19		0.15	0.22–0.75	0.36	0
$1f_{7/2}$	3.71	4.33	3.36	6.0	5.56	4
$1f_{5/2}$	2.17		1.13	1.28–1.72	0.78	6
$2p$	5.37	5.12	6.63	6.84	6.08	6
$3s_{1/2}$	0.072[h]	0.026	0.05	0.24	0.21	2

[a]Present work.
[b]Rapaport *et al.* [2].
[c]Rapaport *et al.* [12].
[d]Rapaport *et al.* [13].
[e]Chowdhury and Sen Gupta [14].
[f]Simple shell model values.
[g]Using levels up to $E_x \sim 3.1$ MeV.
[h]Using levels beyond $E_x \sim 4.8$ MeV.

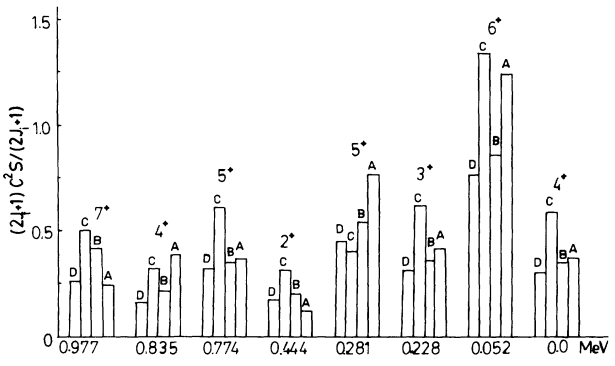

FIG. 10. The measured transition strength compared to the $(f_{7/2})^n$ theory. A, MBZ theory; B, (d,p) reaction, present work; C, (d,p) reaction, Rapaport *et al.*; D, (t,d) reaction, Bing *et al.*.

low-lying levels with $J^\pi=0^+-7^+$ in ^{46}Sc is generated, having the configuration $[\pi(f_{7/2})\nu(f_{7/2})]$, the 0^+ member of which is too weak to be observed. All the other levels ($j^\pi=1^+-7^+$) are identified and populated in the (d,p) and (t,d) reactions on ^{45}Sc, including two 4^+ and two 5^+ levels as predicted by the model. The 0.280 MeV level is the 5^+ level. The spectroscopic factors are also calculated by the MBZ model [15] for the neutron stripping reaction to the $1f_{7/2}$ shell. These are compared with the experimental results (present work and Refs. [2] and [3]) in Fig. 10. The summed strengths, $\sum(2J_f+1)C^2S/(2J_i+1)$, are 3.9, 3.3, 4.7, and 2.7 given, respectively, by the theory, present work, Rapaport *et al.* [2], and Bing *et al.* [3]. The above value of Bing *et al.* is with the bound state geometries of $r_0=1.25$ fm and $1=0.65$ fm, while it becomes 3.4 with $r_0=1.20$ fm, $a=0.65$ fm. All the experimental results are thus, within limits of uncertainty, in agreement with the theory [15].

B. The $l=1$ transitions

A large number of levels (over one hundred up to $E_x\sim7$ MeV), many more than by Rapaport *et al.* [2], is observed in the present work with the characteristic of $l=1$ transfer, but with no sharp division or distinction between the $2p_{3/2}$ and $2p_{1/2}$ states. The distribution of strength (Fig. 9), however, indicates as though two Gaussian patterns are peaked at $E_x\sim2.3$ and ~4 Mev, with a good amount of overlap, and this difference is in excellent agreement with the $2p_{1/2}$-$2p_{3/2}$ separation (~1.8 MeV) in the isotonic nuclei ^{44}Ca and ^{46}Ti (Refs. [12] and [14]). This would indicate that the residual n-p interaction, although it leads to a heavy fragmentation of the strength in the ^{45}Sc(d,p)^{46}Sc reaction, does not affect the position of the shell model state. As in Ref. [2], all $l=1$ transitions were treated together. The summed $2p$ transition strength is 5.4, being in excellent agreement with the single particle value 6. There is a large number of very weak $l=1$ states at high excitation (Fig. 9) and it appears that almost the entire (if not the entire) strength is reached. The spectroscopic factor obtained in the present work level by level, as mentioned earlier, is smaller than that of Rapaport *et al.* [2], but the summed strength is larger as many more $l=1$ transitions are observed by us.

Some of the measured angular distributions are shown in Fig. 5 and compared with the $l=1$ DWBA curves. A reasonably good fit is obtained practically over the entire angular range.

C. The $l=0$ transitions

A few weak $l=0$ transitions were observed. Some of the angular distributions are shown in Fig. 6. The $3s_{1/2}$ shell model state is known to be about 5 MeV above the $1f_{7/2}$ shell [16]. All $l=0$ transitions below $E_x\sim3.1$ MeV were therefore assumed to correspond to the $2s_{1/2}$ shell and those at higher excitation energies ($E_x>4.8$ MeV) to the $3s_{1/2}$ state. An insignificant portion of the $3s_{1/2}$ strength (only about 4%) is reached up to $E_x\sim7$ MeV.

Tentative $l=3$ and 1 assignments were made by Rapaport *et al.* [2] for transitions, respectively, to the levels at $E_x=1.143$ and 1.441 MeV, both of which are found to exhibit an $l=0$ character in our work. The $l=0$ transfer to the latter level is in disagreement with the tentative $J^\pi=2^+$ assignment [1] to the level at $E_x=1.428$ MeV. The assignment of odd parity in our work is consistent with the doublet nature of the level, suggested in the Nuclear Data Sheets [1] from a consideration of the ^{46}Ti(t,^{3}He) and ^{48}Ti(d,α) reactions [17,18], as well as with the odd parity given in a recent (d,α) work [19]. The spin assignment from the present work is, however, inconsistent with the J^π value 2^- of Bamber *et al.* [19]. The situation is thus wrought with conflict.

The present work confirms the $l=0$ assignment to most of the levels below $E_x\sim4$ MeV made in the previous (d,p) reaction [2], and suggests $J^\pi=3^-,4^-$ to some others above $E_x>4$ MeV (Table I), namely $E_x=4.793$, 5.146, 5.343, and 5.561 MeV.

D. The $l=2$ transitions

Four $l=2$ transitions were observed in the present investigation, all below $E_x\sim5$ MeV, and are attributed to the $1d_{3/2}$ hole state. Thus the core excitation effect, including the $2s_{1/2}$ state mentioned above, is observed in the present study. Rapaport *et al.* [2] in their ^{45}Sc(d,p) reaction at $E_d=7$ MeV did not observe any $l=2$ level up to $E_x\sim6$ MeV.

The $l=2$ assignment to the levels at $E_x=2.594$ and 2.651 MeV (Fig. 7) in the present investigation is in disagreement with the tentative $l=0$ assignment of Rapaport *et al.* [2]. Of the other two levels, namely, $E_x=4.153$ and 4.928 MeV, with $l=2$ character in the present work, the former was not populated in their experiment, while the angular distribution of the latter was not measured.

E. General comments

Comments on some of the levels are made below.

The 1.326 meV level as mentioned earlier has an $l=3$ assignment in the present work (Fig. 3) and $l=(1)$ in Ref.

[2], both of which are consistent with the $J^\pi=3^+,(4^+)$ adopted in the Nuclear Data Sheets [1]. The J^π value of the level is variously quoted as $2^+,3^+,4^+,0^-,1^-,2^-,4^-$ in $(d,^3\mathrm{He})$, $(t,^3\mathrm{He})$ and $(\vec{n},\gamma)$ reactions [17,18,20]. The 2^- assignment has recently been made by Bamber *et al.* [19] from the polarized $(\vec{d},\alpha)$ reaction. The level thus appears to be a doublet, one or the other member of which is preferentially populated in the different reactions.

An odd J, positive parity is suggested for the 1.399 MeV level in the $(\vec{d},\alpha)$ reaction [19], while an earlier (d,α) reaction [18] assigns $J^\pi=3^-,(4^-,5^-)$. The $(t,^3\mathrm{He})$ reaction [17] in contradiction to the above two gives $J^\pi=2^+$, which is adopted by Alburger [1]. The (d,p) reaction gives $l=1$ thus confirming the positive parity of the level, although the spectroscopic factors are different by an order of magnitude in the two experiments (present work and Ref. [2]). The level clearly cannot be a singlet; even then the contradiction in the two (d,α) reactions [18,19] is difficult to understand.

The J^π value of the 1.852 MeV level is given as 1^+ from the $(p,^3\mathrm{He})$, $(t,^3\mathrm{He})$, and (d,α) reactions [17,18,21] and adopted in the data sheets [1]; $J^\pi=1^+,2^+$ are suggested in the $(^3\mathrm{He},t)$ reaction [22]. The level is weakly populated in the (d,p) reaction. The present work gives an $l=1$ transfer (nonstripping in Ref. [2]) thus supporting the $J^\pi=2^+$ assignment.

The spin of the 3.064 meV level is given as 2,3,4 in the Nuclear Data Sheets. The level is fairly strong in the (d,p) reaction and the $l=1$ assignment is thus consistent with the above J value and a positive parity is suggested in our work.

All $l=3$ levels, $E_x<1$ MeV, excited in the $(d,^3\mathrm{He})$ reaction [23], are also observed in the (d,p) reaction (present work and Ref. [2]). The most likely configuration of these levels is thus $(1f_{7/2})^6$. However, the 1.121 MeV level found in the $(d,^3\mathrm{He})$ reaction with $l=3$ transfer poses a problem. The level cannot be identified with the 1.124 MeV level adopted in the Nuclear Data Sheets with $J^\pi=4^-$. The l value is in disagreement with the $J^\pi=3^-,4^-$ given in the thermal (n,γ) reaction [20], as well as with the $l=0$ value observed in the two (d,p) reactions (present work and Ref. [2]) for $E_x=1.131$ MeV. It is possible that the level ($E_x=1.121$ MeV of Ref. [23]) is identical with the 1.141 MeV level weakly populated with a tentative $l=3$ transfer in the previous (d,p) reaction [2]. But this level in the present work has a clear $l=0$ angular distribution (Fig. 6) as given by repeated data extraction and has a negative parity from the $(t,^3\mathrm{He})$ reaction [17]. The situation thus is confusing. We may note that the level was not observed in the (d,α) and $(^3\mathrm{He},t)$ reactions [18,22]. It cannot be a member of the $(1f_{7/2})^6$ configuration mentioned above. Only three levels were found to have a small admixture of $l=1$ with $l=3$ in the $^{47}\mathrm{Ti}(d,^3\mathrm{He})$ reaction [23], thus showing the presence of an excited $2p$ proton configuration, however small, in the low-lying level spectrum of ^{46}Sc.

It is interesting to note that the $l=0$ and 2 levels populated in the above $(d,^3\mathrm{He})$ reaction fairly strongly are all weakly populated in the (d,p) reaction (present work and Rapaport *et al.* [2]). From the systematics of the negative parity levels in ^{46}Sc, rotational bands are proposed [24] with $k=1$ and 4. These two bands arise, respectively, from the antiparallel and parallel coupling of the odd neutron in the $\Omega_n=\frac{5}{2}^-[312]$ and the odd proton in the $\Omega_p=\frac{3}{2}^-[202]$ Nilsson orbits with the levels at 0.143 and 0.627 MeV as the bandheads.

V. CONCLUSIONS

The energy levels in ^{46}Sc are obtained up to $E_x\sim7$ MeV and several new levels are identified at high excitation energies. The orbital angular momentum transfers are obtained from the DWBA analyses of the measured angular distributions of a large number of levels, including many not hitherto studied, thus giving the parity of the levels, the J limits and the spectroscopic factors. The spectroscopic factor, level by level, is usually less than that of Rapaport *et al.* [2]. The spectroscopic strengths are heavily fragmented. The $1f_{7/2}$ strength, for example, in the (d,p) reaction on the isotonic nuclei ^{44}Ca and ^{46}Ti is, respectively, carried by a single level and by five or six levels. A good amount of the $2p_{3/2}$ strength is concentrated on a single level in ^{45}Ca and ^{47}Ti, whereas no such level is found in ^{46}Sc with an overwhelming strength.

The $2p$ and $1f_{7/2}$ strengths in the $^{45}\mathrm{Sc}(d,p)$ reaction have probably been exhausted and about 30–40 % of the $1f_{5/2}$ strength is reached. The $3s_{1/2}$ state has just begun to appear. The negative parity (low-lying) levels are extremely weakly excited in the (d,p) reaction, while they are strongly populated in the $(d,^3\mathrm{He})$ reaction, showing clearly the hole nature of the levels.

ACKNOWLEDGMENTS

The authors wish to thank Professor P. D. Kunz for the DWUCK4 program and Professor K. W. Allen and Dr. D. Roaf for their interest in the work. They are thankful to Dr. F. Watt and Dr. M. J. Hurst for help with the exposure at Oxford. One of the authors (H.M.S.G.) acknowledges financial support from the Royal Society, London while doing the experiment at Oxford.

[1] D. E. Alburger, Nucl. Data Sheets **49**, 237 (1986).
[2] J. Rapaport, A. Sperduto, and W. W. Buechner, Phys. Rev. **151**, 939 (1966).
[3] O. Bing, G. Bonneaud, D. Magnac-Valtett, and C. Gerardin, Nucl. Phys. **A257**, 460 (1976).
[4] H. M. Sen Gupta, J. B. A. England, E. M. E. Rawas, F. Khazaie, and G. T. A. Squier, J. Phys. G **16**, 1039 (1990).
[5] K. K. Seth, J. Picard, and G. R. Satchler, Nucl. Phys. **A140**, 577 (1970).
[6] P. Schwandt and W. Haeberli, Nucl. Phys. **A123**, 401 (1969).
[7] G. Brown, A. Denning, and A. E. Macgregor, Nucl. Phys. **A153**, 145 (1970).
[8] W. Fitz, J. Heger, R. Santo, and S. Wenneis, Nucl. Phys.

A143, 113 (1970).
[9] J. C. Lombardi, R. N. Boyd, R. Arking, and A. B. Robins, Nucl. Phys. **A188**, 103 (1972).
[10] F. D. Becchetti, Jr. and G. W. Greenless, Phys. Rev. **182**, 1190 (1969).
[11] H. Banu, H. M. Sen Gupta, and F. Watt, Nucl. Phys. **A378**, 11 (1982).
[12] J. Rapaport, W. E. Dorenbusch, and T. A. Belote, Phys. Rev. **156**, 1255 (1967).
[13] J. Rapaport, A. Sperduto, and W. W. Buechner, Phys. Rev. **143**, 808 (1966).
[14] M. S. Chowdhury and H. M. Sen Gupta, Nucl. Phys. **A229**, 484 (1974).
[15] J. D. McCullen, B. F. Bayman, and L. Zamick, Phys. Rev. **134**, B515 (1964).
[16] H. H. Bolotin, Phys. Rev. **138**, B795 (1965).
[17] F. Ajzenberg-Selove, R. E. Brown, E. R. Flynn, and J. W. Sunier, Phys. Rev. C **32**, 756 (1985).
[18] M. B. Lewis, Phys. Rev. **184**, 1081 (1969); A. Guichard, M. Bedjidian, J. Y. Grossiord, M. Gusakow, J. R. Pizzi, and C. Ruhla, Nucl. Phys. **A192**, 126 (1972).
[19] C. Bamber, N. J. Davis, J. A. Kuehner, A. A. Pilt, A. J. Trudell, M. C. Vetterli, and G. D. Jones, Phys. Rev. C **34**, 1236 (1986).
[20] H. I. Liou, R. E. Chrien, J. Kopecky, and J. A. Konter, Nucl. Phys. **A337**, 401 (1980).
[21] A. Guichard, W. Benensen, R. G. Markham, and H. Nann, Phys. Rev. C **13**, 540 (1976).
[22] J. L. Yntema, Phys. Rev. C **4**, 1211 (1971).
[23] M. B. Lewis, Phys. Rev. C **1**, 501 (1970).
[24] B. B. V. Raju and B. M. Spicer, Aust. J. Phys. **23**, 225 (1970); G. D. Dracoulis, J. L. Drell, and W. Gelletly, J. Phys. A **6**, 141 (1973).